משרד החקלאות - דו"ח לתוכניות מחקר
לקרן המדען הראשי

קוד זיהוי	א. נושא המחקר (בעברית)
11 - 0565 - 838	מערכת רובוטית משולבת אדם לגיזום ועיצוב עצי מטע

	ב. צוות החוקרים

	שם פרטי	שם משפחה	
חוקר ראשי	רפאל	לינקר	
		חוקרים משניים	
1	בכר	אביטל	
2	שמילוביץ	זאב	
3	שמולביץ	יצחק	
4	גרינבלט	יעל	
5			
6			
7			

		ג. כללי
	מוסד מחקר של החוקר הראשי	
	טכניון	

סוג הדו"ח	תאריכים	
מסכם	תקופת המחקר עבורה מוגש הדו"ח	תאריך משלוח הדו"ח למקורות המימון

	התחלה		סיום		שנה	חודש
	שנה	חודש	שנה	חודש		
	2010 / 05		2013 / 10		2014 / 01	

ד. מקורות מימון עבורם מיועד הדו"ח

שם מקור המימון	קוד מקור מימון	סכום שאושר למחקר בשנת תיקצוב הדו"ח בשקלים
מדען ראשי		604,350

ה. תקציר שים לב - על התקציר להיכתב בעברית לפי סעיף ה' שבהנחיות לכתיבת דיווחים

גיזום הינו פעולה המצריכה כוח אדם רב ועל כן הפרויקט הנוכחי התמקד בפיתוח מערכת רובוטית משולבת אדם אשר במסגרתה המפעיל האנושי יבחר את הענפים המיועדים לגיזום וזרוע רובוטית תבצע את המשימה בצורה אוטומטית. הפרויקט שילב שלוש משימות עיקריות: פיתוח כלי החיתוך, פיתוח מודל תלת מימדי של העץ והנחיית הזרוע הרובוטית. האתגר המרכזי היה בפיתוח מודל תלת מימדי של העץ ועיכובים במשימה זו מנעו מאיתנו להשלים את האינטגרציה של המרכיבים השונים עד כדי קבלת מערכת משולבת אחת. יחד עם זאת, חלה התקדמות משמעותית לקראת השגת המטרות והתאפשר לנו להדגים את ייתכנות הגישה המוצעת בסביבה מעבדתית.
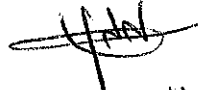
ו. אישורים

הנני מאשר שקראתי את ההנחיות להגשת דיווחים לקרן המדען הראשי והדו"ח המצ"ב ...

Mano Medalsi, CPA
Research Authority

13 -01- 2014		Mano Medalsi		
תאריך (שנה) (חודש) (יום)		מנהל המוסד (פקולטה) (רשות המחקר)	מנהל המחלקה	חוקר ראשי

9.1.2014

8.1.14

דוח לתכנית מחקר מספר 838-0565-11

מערכת רובוטית משולבת אדם לגיזום ועיצוב עצי מטע

Human-robot integrated system for tree pruning and shaping

מוגש לקרן המדען הראשי במשרד החקלאות ולהנהלת ענף פרחים

ע"י

רפאל לינקר	הפקולטה להנדסה אזרחית וסביבתית, טכניון	
אביטל בכר	המכון להנדסה חקלאית, מנהל המחקר החקלאי, בית דגן	
זאב שמילוביץ	המכון להנדסה חקלאית, מנהל המחקר החקלאי, בית דגן	
יצחק שמולביץ	הפקולטה להנדסה אזרחית וסביבתית, טכניון	
יעל גרינבלט	שירות ההדרכה והמקצוע	

Raphael Linker, Faculty of Civil and Environmental Engineering, Technion, Haifa. E-mail: linkerr@tx.technion.ac.il

Avital Bechar, Institute of Agricultural Engineering, Agricultural Research Organization, Bet Dagan, E-mail: avital@volcani.agri.gov.il

Zeev Schmilovitch, Institute of Agricultural Engineering, Agricultural Research Organization, Bet Dagan, E-mail: veshmilo@volcani.agri.gov.il

Itzak Schumevich, Faculty of Civil and Environmental Engineering, Technion, Haifa. E-mail: agshmilo@tx.technion.ac.il

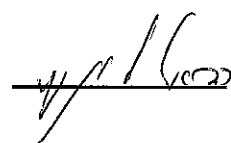Yael Greenwalt, Agricultural Extension Service, E-mail: yael_gr@shaham.moag.gov.il

תקציר

גיזום הינו פעולה המצריכה כוח אדם רב ועל כן הפרויקט הנוכחי התמקד בפיתוח מערכת רובוטית משולבת אדם אשר במסגרתה המפעיל האנושי יבחר את הענפים המיועדים לגיזום וזרוע רובוטית תבצע את המשימה בצורה אוטומטית. הפרויקט שילב שלוש משימות עיקריות: פיתוח כלי החיתוך, פיתוח מודל תלת מימדי של העץ והנחיית הזרוע הרובוטית. האתגר המרכזי היה בפיתוח מודל תלת מימדי של העץ ועיכובים במשימה זו מנעו מאיתנו להשלים את האינטגרציה של המרכיבים השונים עד כדי קבלת מערכת משולבת אחת. יחד עם זאת, חלה התקדמות משמעותית לקראת השגת המטרות והתאפשר לנו להדגים את יתכנות הגישה המוצעת בסביבה מעבדתית.

....

הצהרת החוקר הראשי:

הממצאים בדו"ח זה הינם תוצאות ניסויים.

הניסויים מהווים המלצות לחקלאים: לא

חתימת החוקר

סיכום עם שאלות מנחות

נא להתייחס לכל השאלות בקצרה ולעניין, ב-3 עד 4 שורות לכל שאלה (לא תובא בחשבון חריגה ממגבלות המסגרת המודפסת).

שיתוף הפעולה שלך יסייע לתהליך ההערכה של תוצאות המחקר.

הערה: נא לציין הפנייה לדו"ח אם נכללו בו נקודות נוספות לאלה שבסיכום.

מטרות המחקר תוך התייחסות לתוכנית העבודה.
פיתוח מערכת רובוטית אוטונומית משולבת אדם לגיזום עצי מטע
עיקרי הניסויים והתוצאות.
(1) פותח ונבדק כלי חיתוך מתאים למשימה. (2) פותחו מספר אלגוריתמים לבניית מודל תלת מימדי של עץ על בסיס תמונות צבע ו/או תמונות עומק (range images). (3) פותחו ונבחנו אלגוריתמים להנחיית הזרועות הרובוטיות במכון וולקני ובטכניון. פותחו ונבחנו אלגוריתמים לשיתוף אדם במערכת הגיזום הרובוטית.
מסקנות מדעיות והשלכות לגבי יישום המחקר והמשכו. האם הושגו מטרות המחקר לתקופת הדוח?
פותחו האלגוריתמים ושיטות העבודה לגיזום רובוטי משולב אדם. נדרשת עוד עבודה משמעותית עד לקבלת אב טיפוס המתאים לעבודה במטע אך תוצאות המחקר מוכיחות על היתכנות של הגישה המוצעת
בעיות שנותרו לפתרון ו/או שינויים (טכנולוגיים, שיווקיים ואחרים) שחלו במהלך העבודה; התייחסות המשך המחקר לגביהן, האם יושגו מטרות המחקר בתקופה שנותרה לביצוע תוכנית המחקר?
קשיים בבניית המודל התלת מימדי של העץ גורמו לעיכובים שמנעו אינטגרציה של הרכיבים השונים שפותחו במסגרת המחקר. יחד עם זאת הרכיבים השונים של המערכת הודגמו בעזרת מערכת מעבדתית
הפצת הידע שנוצר בתקופת הדו"ח: **פרסומים בכתב** - <u>ציטוט</u> ביבליוגרפי כמקובל בפרסום מאמר מדעי; **פטנטים** - יש לציין שם ומס' פטנט; **הרצאות וימי עיון** - יש לפרט מקום, תאריך, ציטוט ביבליוגרפי של התקציר כמקובל בפרסום מאמר מדעי.
העבודה תוצג בכנס AGENG2014 בצוריך שווייץ
פרסום הדוח: אני ממליץ לפרסם את הדוח: (סמן אחת מהאופציות)
◄ ~~רק בספריות~~
◄ ללא הגבלה (בספריות ובאינטרנט)
◄ ~~חסוי לא לפרסם~~
האם בכוונתך להגיש תוכנית המשך בתום תקופת המחקר הנוכחי? כן - לא -

*יש לענות על שאלה זו רק בדוח שנה ראשונה במחקר שאושר לשנתיים, או בדוח שנה שניה במחקר שאושר לשלוש שנים

Abstract

Pruning is one of the most labor-intensive tasks performed in orchards and could greatly benefit from the introduction mechanization and automation. The aim of the present project was to develop a semi-automated, human-integrated system in which the user would select the branches that require pruning and a robotic arm would perform the operation automatically. The project was organized in three main tasks: development of an appropriate cutting tool, three-dimensional modeling of the tree and guidance of the robotic arm. The most challenging tasks proved to be the modeling task and delays in this task have prevented us from completing the integration of the various components into a combined system. Nonetheless, major progress was made toward the achievement of the initial goal and we were able to demonstrate the feasibility of the proposed approach in a laboratory environment.

1.   Introduction

Pruning is one of the most labor-intensive tasks performed in orchards and significant savings in terms of manpower could be achieved through mechanization and automation of this task. The aim of the present project was to develop a semi-automated, human-integrated system in which the user would select the branches that require pruning and a robotic arm would perform the operation automatically. Due to their specific shape (see Section 4), nectarine trees were selected as case study. The development of such a system involved three main tasks which are detailed in Section 2-4. Section 5 presents a first step toward the integration of the various components into a single system.

2.   Cutting tool

A cutting tool was developed for pruning branches with diameter of up to 26mm at 45° cutting angle. Several cutting tools were investigated and are elaborated in the 1st year report. The maximum cutting diameter was determined based on a measurement of 238 nectarine branches in the field using a Caliber. A histogram of the branches diameter was generated in order to examine the branches diameter distribution (Figure 1).
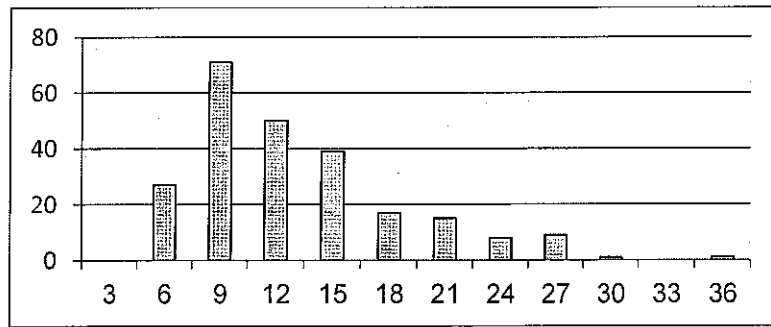
Figure 1: Branches diameter distribution.

The maximum branch diameter was 36mm and in order to be able to cut most of the branches and maintain minimal dimensions of the tool, it was determined that the tool will cut branches with diameter of up to 26mm which correspond to 98% of the branches. Based on this and the following equation $= \emptyset = 2 \cdot b + \emptyset shaft$, the saw diameter should be 115mm with standard shaft diameter of 41mm. The cutting tool prototype was tested manually in the field (Figure 2) and then mounted on the end effector of a Motoman 5L manipulator in the Agricultural Robotics Lab (ARL) at Volcani Center (see Section 5).
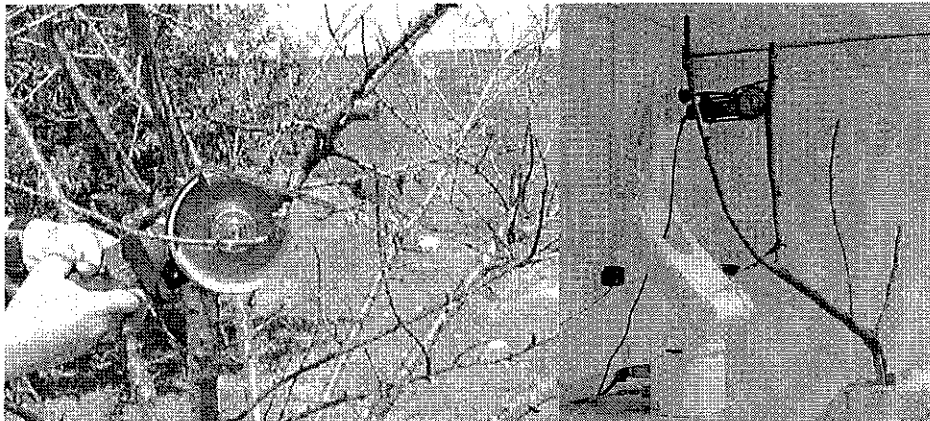
Figure 2: Cutting tool test in the field and mounted on the Motoman manipulator

3.   Modeling

Obtaining an accurate three-dimensional model of the tree is a key-element required for the interaction between the proposed system and the user as well as for planning the trajectory of the robotic arm. Due to the importance of this topic we investigated three approaches:

3.1   Modeling based on images from multiple viewpoints

One way to obtain a 3D model of a 3D object is to use several 2D images of this object acquired from different viewpoints. Most existing methods require calibrated images or little disparity between the views (and hence a large number of images).

Such requirements cannot be easily met for the current application. This led us to investigate the method developed by Lhuillier and Quan (2005), which reconstructs 3D objects from uncalibrated images. The main steps of this algorithm are:

1. Detect "points of interest" in each image. Establish the initial correspondences between the images by computing normalized correlation. Sort the validated correspondences by correlation score and use them to initialize a list of seed matches for match propagation.

2. Apply "unconstrained propagation" from all the seed points using a best-first strategy without the epipolar constraint in order to obtain quasi-dense pixel correspondences represented as a disparity map.

3. Resample the quasi-dense disparity map by local homographies to obtain quasi-dense (subpixel) point correspondences. Estimate the fundamental matrix using a standard robust algorithm on the resampled points.

4. Apply constrained propagation from the same initial list of seeds using a best-first strategy with the epipolar constraint expressed by the computed fundamental matrix.

5. Resample the obtained disparity map to get the final quasi-dense point correspondences.

Figure 3 shows sequences of images in which the "points of interest" are indicated by "+" symbols. Figure 4 shows the quasi-dense map obtained after applying unconstrained propagation. This quasi-dense map is resampled by local homographies and the result is shown in Figure 5. Using this quasi-dense map, the fundamental matrix that will enable combining the images to obtain the 3D model can be determined (on-going work).
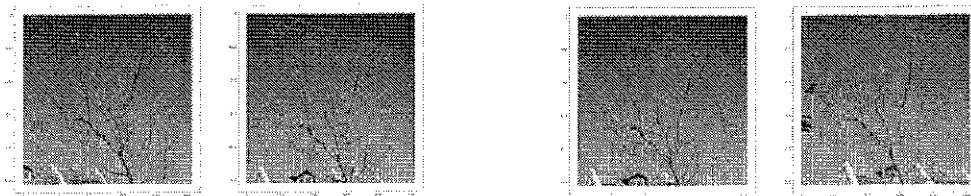

Figure 3: First step toward 3D model based on images from multiple viewpoints: Sequences of images in which the "points of interest" are indicated by "+" symbols
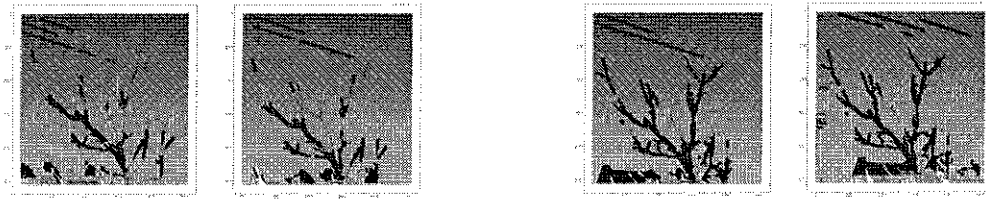
Figure 4: Second step toward 3D model based on images from multiple viewpoints: Quasi-dense map obtained after applying unconstrained propagation
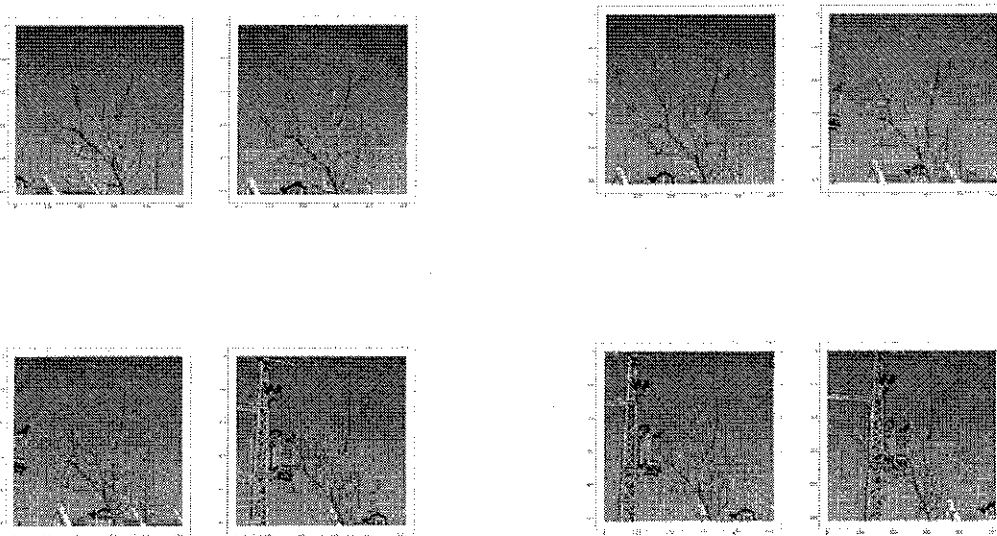
Figure 5: Third step toward 3D model based on images from multiple viewpoints: images resampled by local homographies

3.2   Modeling based on 3D clouds from multiple viewpoints

Three-dimensional clouds of points (range images) can be obtained directly using stereoscopic vision or 4D sensors such as time-of-flight (TOF) cameras. Preliminary investigation with a stereoscopic camera yielded poor results and during the second part of the project we focused on the use of a Microsoft Kinect (which relies on projected infrared patterns) for demonstration purposes. Most of the existing techniques for modeling 3D objects from range images rely on detecting local plane direction and keypoints, and merging the information from several images into one global model. These methods require low noise images with strong patterns for the keypoints. In our case the noise level was too high and the bark pattern was too weak to use these techniques "as is" and we are still developing improved algorithms.

The tree is modeled by a connected set of cylinders in 3D space, with some a-priori distribution of its properties (branch length and thickness etc.). Tree detection is the process of finding the model parameters that best approximates a given set of range images. However, due to the complexity of the tree geometry, a whole branch cannot be detected directly and we introduce the Cylindrical Surface Element (CSE), which is part of a branch surface. It is part of the surface of a cylinder and has the following properties:

◆ It is defined by the center point and orientation of the axis of the cylinder it belongs to, its length, radius, and the angular span of the surface that it covers

◆ It can be detected directly by matching a CSE to a set of neighboring points

◆ It can be detected in point clouds resulting from a single range image as well as these resulting from several range images

◆ Its length is larger than typical branch diameter so that it has distinctive direction.

◆ It will be curved towards the camera, and relatively normal to it.

The algorithm steps are:

1. In each range image I:

1.1.   Match a surface element to each point and reject the elements where the approximation error is beyond a certain limit.

1.2.   Using local non-maxima suppression, select a set of surface elements with maximal match (minimal error) and small overlap. This set of elements describes best the visible parts of the tree in image I with minimal approximation error.

2. For all surface elements, use generalized Hough transform to find cylinders.

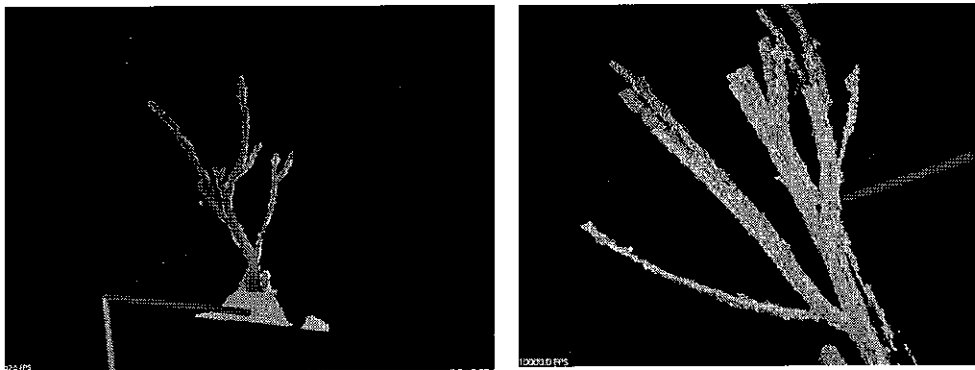Typical result of Steps 1.1 and 1.2 are shown in Figure 6. Step 2 is still under development.

Figure 6: Example of 3D tree model created from range images from multiple viewpoints

3.3   Close-up modeling based on laser scanning

The approaches described in the previous sections cannot identify small branches with an accuracy that would be sufficient to guide the pruning implement to the cutting position. For this high resolution local modeling we investigated the use of a camera and planar laser mounted on the end-effector (Figure 7).
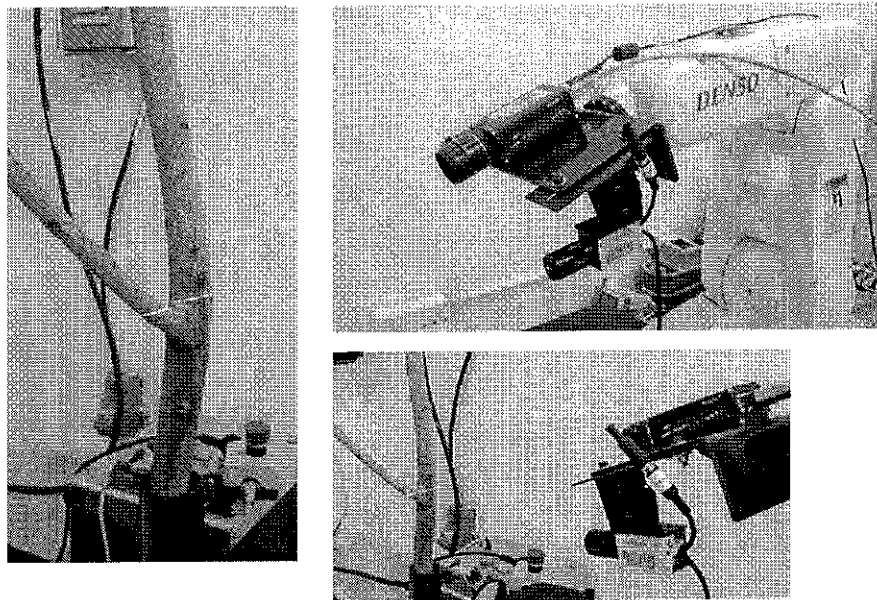
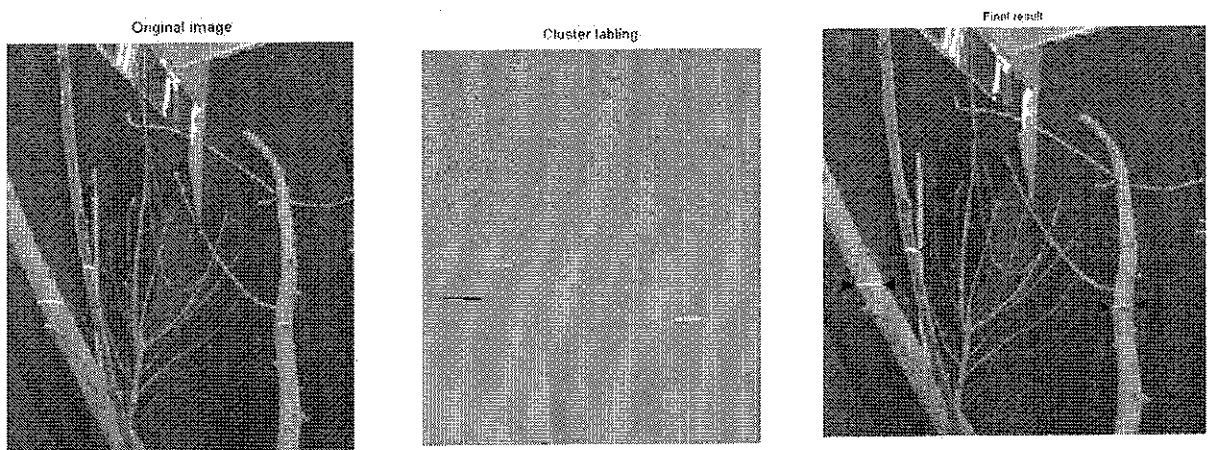Figure 7: Camera and planar laser system mounted of the end effector

Figure 8: Left - Image acquired by the camera mounted on the end effector, showing the laser plane intersecting the branches. Middle – Cluster corresponding to extracted laser lines. Right – Identified cluster shown on branches

The extraction of the laser line was performed in the CIE-LAB color space which is less sensitive to illumination fluctuations than the RGB representation. This color-

based extraction was followed by a morphologic test based on the fact that the system was designed in such a way the laser produces a horizontal line on a planar object perpendicular to the camera principal axis. Typical results are shown in Figure 8. The endpoints of the laser segments in the image plane is transformed into a fixed global coordinate system using (1) the relative position between the laser and the camera and (2) the homogenous transformation matrix of the robot. After applying this transformation to the endpoints of all segments, the middle point of each segment is calculated. Since the imaging system typically retrieves a 150° arc from the circumference of a branch, simple geometry considerations show that this midpoint is very close to the actual center of the branch.

Collecting all the clusters midpoints, we obtain a 3D point cloud representation of the skeleton of the tree (Figure 9). This point cloud is transformed into a vector point cloud in which each point has its heading as additional characteristic. Finally, recursive clustering is used to group these points into clusters that correspond to the actual branches (Figure 9).
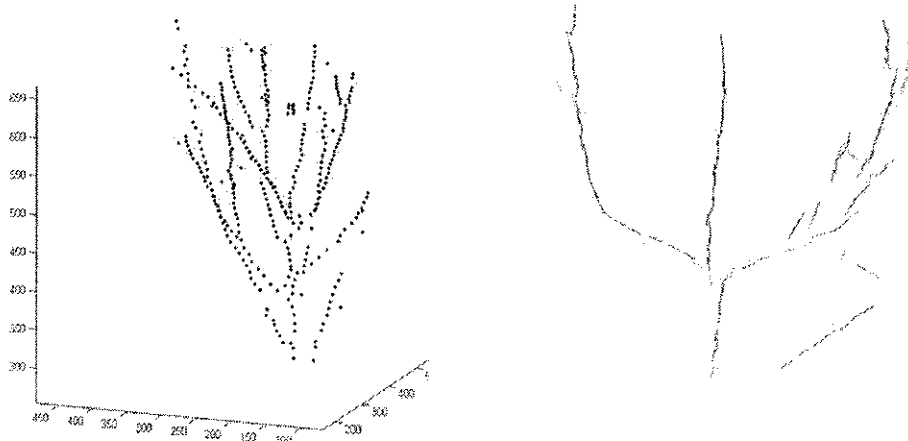
Figure 9: Left - 3D point cloud representation of the skeleton of the tree. Right – Example of tree skeleton after forming clusters corresponding to branches.

After completing the clustering operation the next step is to determine how the clusters are related to each other and to determine the branch hierarchy. A typical result is shown in Figure 10, which shows that if the user requires to prune branches 2, 6 and 7, the system determines that this requires pruning only branches 6 and 7.
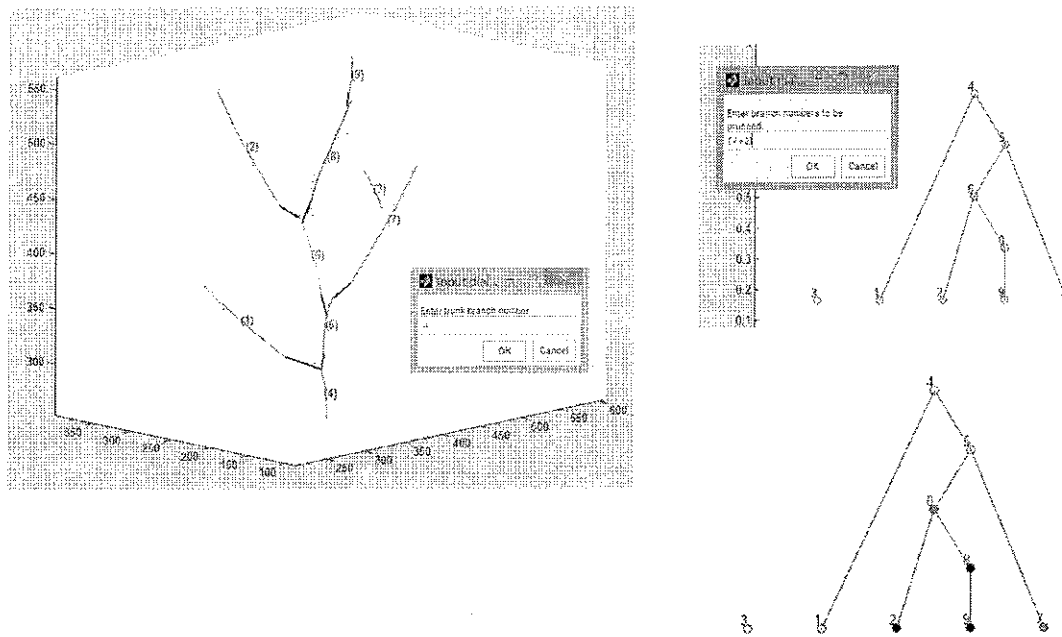
Figure 10: Left - 3D point cloud representation of the skeleton of the tree. Right – Example of tree skeleton after forming clusters corresponding to branches.

4. Fast motion along a branch using visual servoing

As mentioned in the Introduction, nectarine trees were selected as case study. Such trees have a typical "cup" shape with four or five main branches distributed more or less evenly along the circumference (Figure 11). For such trees the pruning operation must remove all the branches growing "inside the cup" and some of the branches growing outwards. Due to this special requirement, an alternative to the standard motion control approach presented in the previous section could be as follows: (1) starting at the bottom of a main branch the pruning arm moves along the branch, inside the cup, and removes all branches growing inwards; (2) once the pruning arm reaches the top of the main branch it comes back toward the bottom of the branch and during this second pass it prunes the selected outward-growing branches. Such an approach requires a feedback control system that enables the pruning arm to move at high speed along a curved branch, and the present section reports the development of such a system.
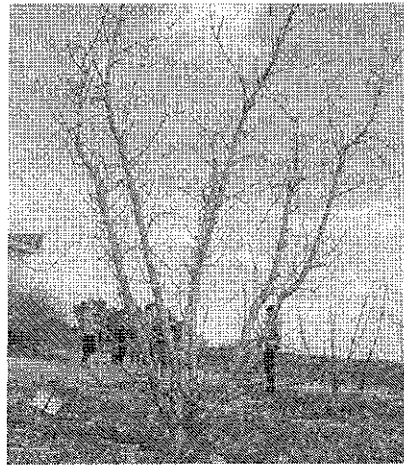
Figure 11: Typical nectarine tree

Manual sampling of a number of trees performed at the beginning of the project showed that the main branches have a diameter ranging from 7 to 10cm and the secondary branches have a diameter ranging from 0.3 to 4.0cm. A servoing system based on these characteristics was developed and tested in the laboratory using artificial "branches" created with Platsiv material.

Generally speaking visual servoing can be achieved either using a fixed camera that sees both the robotic arm and the target, or using a camera mounted near the end-effector of the arm (Figure 12). We adopted the second approach and installed a small camera at the end-effector of the robotic arm (similar to Figure 7).
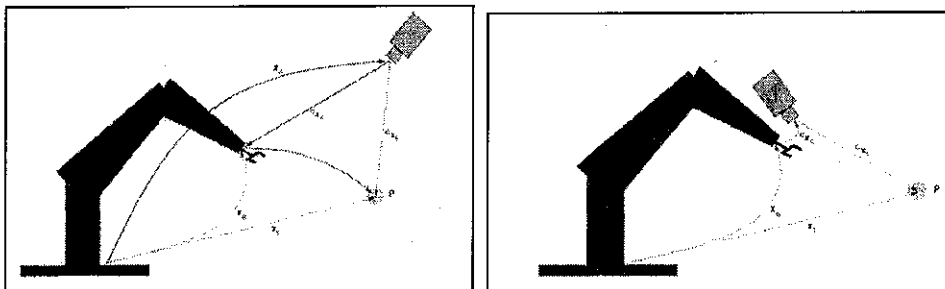
Figure 11: Visual servoing configuration

Figure 12 shows a typical image acquired by the camera and illustrates the main steps of the visual servoing procedure:

1.   Correct optical aberrations, which is done via off-line calibration of the imaging system

2.   Reduce the size of the image to ensure fast computations. Only the Red channel of the image is used and the image is down-sampled from 640*480 to 320*240 pixels

3.   Apply thresholding and extract the boundaries of the branches. After completing this step the branches boundaries are close to straight lines.

4.   Use Hough transform to retrieve the characteristics of the main branch, i.e. the parameters that define the boundaries of the branch in polar coordinate system

$$S = (\rho_L, \theta_L, \rho_R, \theta_L,)$$

		2	
θ [deg]		-8.5	
ρ [pixel]		91	
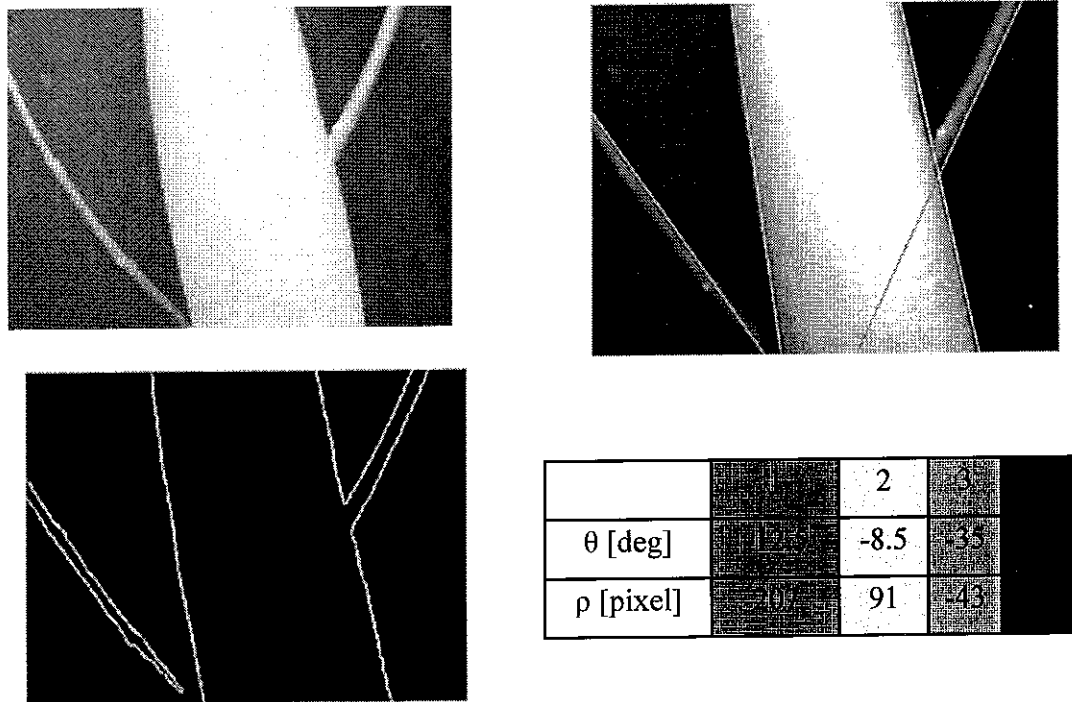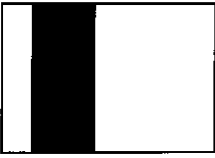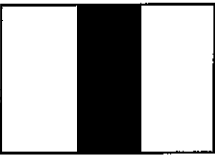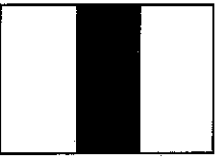
Figure 12: Top left – Image acquired by the end effector camera. Bottom left – Edges extracted after correcting optical aberrations. Top right – Corrected images with superposed identified edges. The table lists the parameters of the extracted edges (polar coordinates). The direction to be followed corresponds to the edges 1 and 2 which have similar θ. The distance between the these two edges (difference in ρ) is a function of the distance between the camera and the cylinder.

A feedback control law was developed following the approach described by Chaumette (1990) and Espiau and Chaumette (1992). According to this approach maintaining a fixed distance between the end-effector of the robotic arm (camera) and the branch (cylinder) is achieved by ensuring that the parameters extracted from the

image $S = (\rho_L, \theta_L, \rho_R, \theta_R,)$ are equal to the reference values that correspond to the desired position $S^{Ref} = \left(\rho_L^{Ref}, \theta_L^{Ref}, \rho_R^{Ref}, \theta_R^{Ref}\right)$. The position of the camera is controlled via six velocities: three translational velocities $\bar{v} = \left(T_x, T_y, T_z\right)$ and three rotational velocities $\bar{\omega} = \left(\omega_x, \omega_y, \omega_z\right)$. A full description of the mathematical relationships between these velocities and the "image parameters" $S = (\rho_L, \theta_L, \rho_R, \theta_L,)$ is not presented here but Figure 13 summarizes these relationships and shows how $\bar{v}$ and $\bar{\omega}$ can be used to bring $S = (\rho_L, \theta_L, \rho_R, \theta_R,)$ to the desired reference values $S^{Ref} = \left(\rho_L^{Ref}, \theta_L^{Ref}, \rho_R^{Ref}, \theta_R^{Ref}\right)$. Clearly, there are two degrees of freedom which are not controlled via $\bar{v}$ and $\bar{\omega}$: the longitudinal velocity along the cylinder and the rotational velocity in a plane perpendicular to the cylinder axis. It is easy to see that the image parameters $S = (\rho_L, \theta_L, \rho_R, \theta_L,)$ are insensitive to these velocities. These velocities must be set a priori based on the desired motion: For instance, assuming that the distance and the angle between the start-point and the end-point are known and that the time allocated to perform the move is set, these two velocities can be calculated.
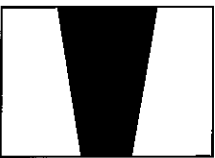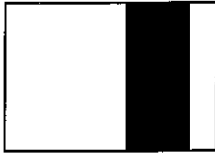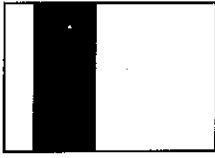
Figure 13: Graphical description of the relationships between the velocities of the arm articulations and the parameters extracted from the images. The position of the end-effector is controlled via six velocities: three translational velocities $\bar{v} = (T_x, T_y, T_z)$ and three rotational velocities $\bar{\omega} = (\omega_x, \omega_y, \omega_z)$. "+" and "-" denote the direction of motion and indicate increase or decrease of the corresponding parameter. ".." indicates that the parameter is not affected by the motion.

The results of five experimental runs in which the pruning arm moved from the starting position to the first branch to be pruned, paused for a few seconds and moved to the second branch to be pruned are presented in Figures 15-19. The velocity profiles prescribed for the two velocities not controlled via visual servoing feedback are listed in Table 1. Figure 15 shows the results for a straight cylinder, Figures 16 and 17 show the results for a curved cylinder (two runs corresponding to the camera facing the curvature head on and from the side) and Figure 18 and 19 show the results for a S-shape cylinder (two runs corresponding to the camera facing the curvature head on and from the side). All three set-ups are shown in Figure 14. These shapes and curvature radii were based on measurements on nectarine trees.
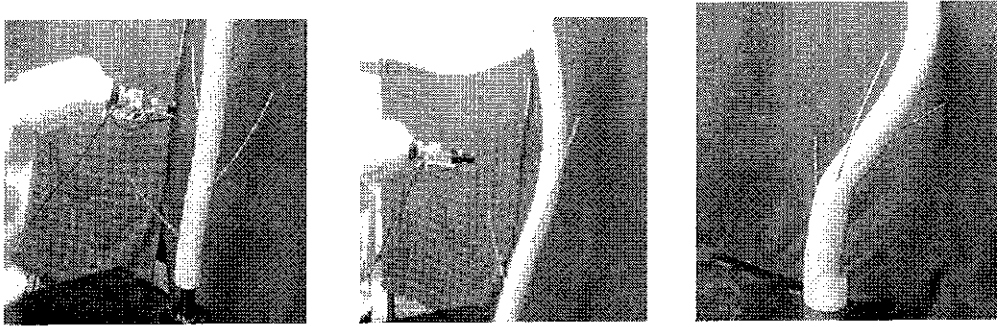

Figure 14: Artificial branches used to test the visual servoing system

Table 1: Velocities imposed during the tests

		Time [s]	Vx [cm/s]	Vy [cm/s]	dx [cm]	dy [cm]
Run 1	Part 1	5	$\pi/3$	3	5.23	15
	Part 2	3	0	5	0	15
Run 2	Part 1	5	$\pi/3$	3	5.23	15
	Part 2	3	0	5	0	15
Run 3	Part 1	5	$\pi/3$	3	5.23	15
	Part 2	5	0	3	0	15
Run 4	Part 1	5	$\pi/3$	3	5.23	15
	Part 2	2	0	5	0	10
Run 5	Part 1	5	$\pi/3$	3	5.23	15
	Part 2	2	0	5	0	10

It can be seen that in all runs with the straight and curved cylinder the image parameters $S = (\rho_L, \theta_L, \rho_R, \theta_R)$ extracted from the images converged smoothly toward their desired values, with very small tracking errors. In the runs with the S-shaped cylinder the feature extraction algorithm failed for short period of time (only one boundary of the cylinder was identified in the image) but the system remained stable and was able to overcome this temporary lack of information.
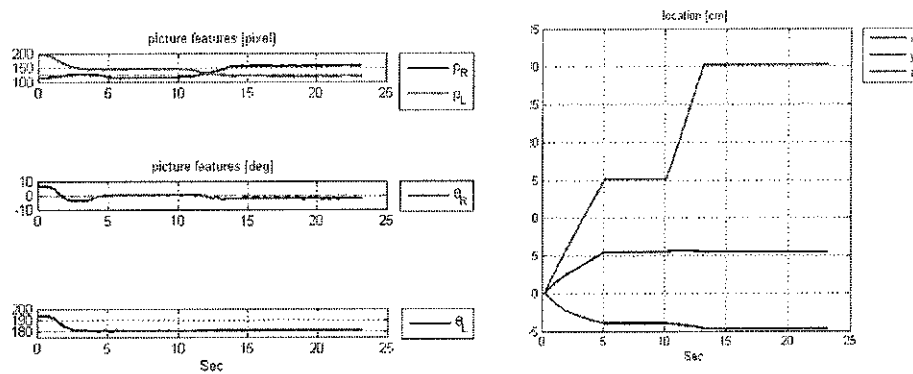
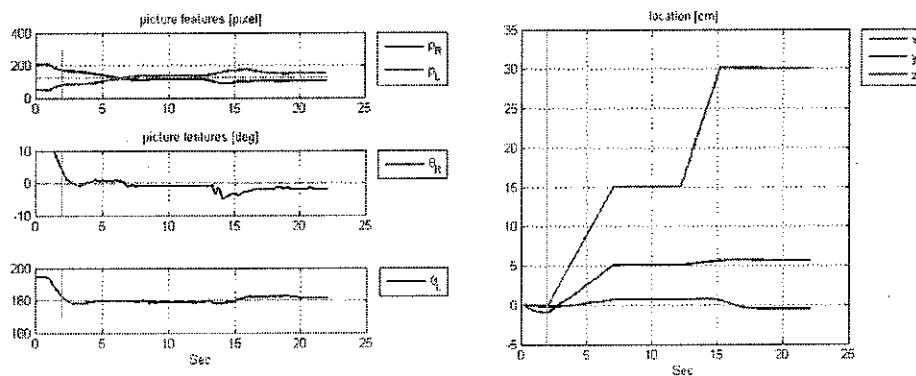Figure 15: Experimental test of the visual servoing system. Run 1 – Straight cylinder

Figure 16: Experimental test of the visual servoing system. Run 2 – Curved cylinder with camera facing the curvature head-on
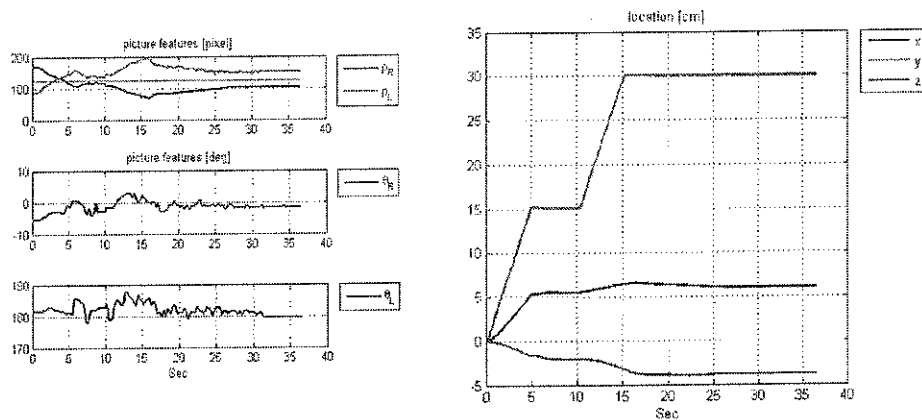
Figure 17: Experimental test of the visual servoing system. Run 3 – Curved cylinder with camera facing the curvature from the side
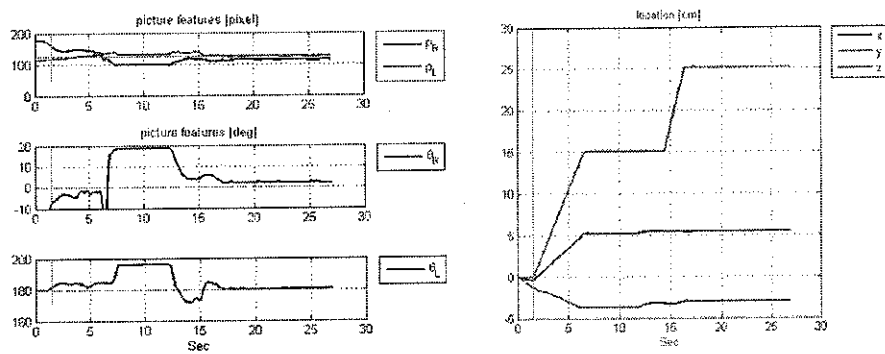

Figure 18: Experimental test of the visual servoing system. Run 4 – S-shaped cylinder with camera facing the curvature head-on
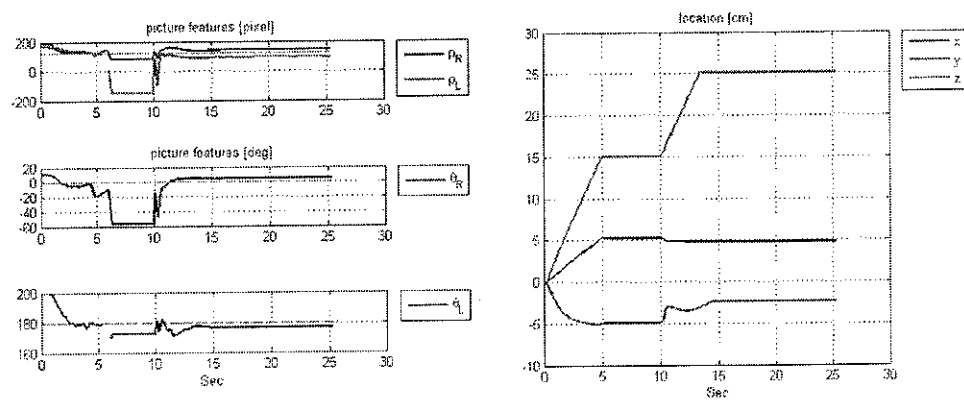

Figure 19: Experimental test of the visual servoing system. Run 5 – S-shaped cylinder with camera facing the curvature from the side

5. Overall system integration

Due to time constraints it was not possible to combine all the components presented above into a single system. The main obstacle was embedding the tree modeling procedure into the control algorithm of the robotic arm. Therefore we conducted a preliminary experiment in which a digitizer developed at ARL was used in order to create a model the examined tree (Figure 20) (instead images or range images from multiple viewpoints). The computerized tree model was used to determine the optimal reaching orientation and visiting order of the desired cutting points (Figure 21). This trajectory optimization was conducted using the 6D configuration space of the robot.
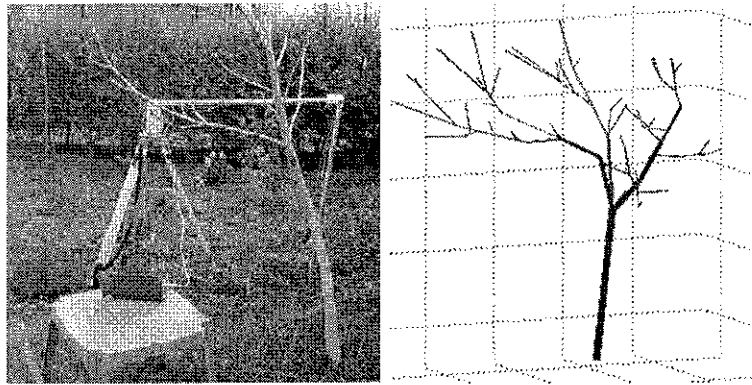

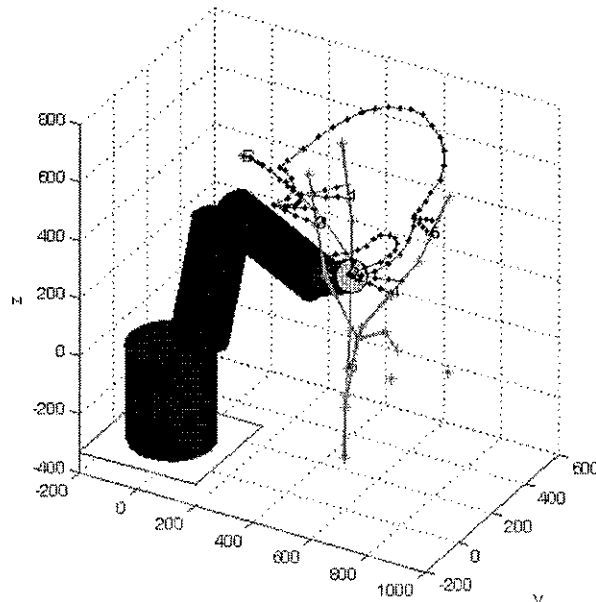Figure 20: Digitizer and tree modeling.

Figure 21: Digitizer and tree modeling.

A visual servoing methodology and a human-robot collaborative system for selective tree pruning were developed. The system consists of a Motoman manipulator, a color

camera, a single beam laser distance sensor, an HMI and a circular saw cutting tool prototype. The cutting tool, camera and laser sensor are mounted on the manipulator's end-effector, aligned parallel to each other (Figure 22).
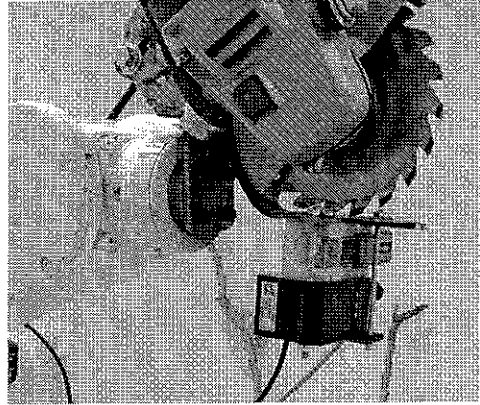

Figure 22: Visual servoing end-effector system.

The system works in two phases. In the first phase, the camera transfer a 2D image of the tree to a human operator which in turn marks on a display the branches to be removed. In the second phase, the system works autonomously: The manipulator maneuvers the laser sensor to measure the branch distance and calculates a trajectory to the cutting point. Once this trajectory has been calculated, the robotic arm performs the corresponding moves and cuts the branch at the prescribed location. Two types of motion planning were investigated, a linear motion between the tool initial location and the cutting point in global Cartesian coordinates and in robot joint space. Laboratory experiments were conducted to investigate the performance of the cutting tool, the Human-Robot system and to compare between the two types of visual servoing motion planning.

6. Conclusions

Pruning is one of the most labor-intensive tasks performed in orchards and could greatly benefit from the introduction mechanization and automation. The aim of the present project was to develop a semi-automated, human-integrated system in which the user would select the branches that require pruning and a robotic arm would perform the operation automatically. The project was organized in three main tasks: development of an appropriate cutting tool, three-dimensional modeling of the tree and guidance of the robotic arm. The most challenging tasks proved to be the modeling task and delays in this task have prevented us from completing the

integration of the various components into a combined system. Nonetheless, major progress was made toward the achievement of the initial goal and we were able to demonstrate the feasibility of the proposed approach in a laboratory environment.

Acknowledgments

- Victor Bloch for 3D modeling of trees and branches using the digitizer, for developing the optimal trajectory using Cspace and for taking part in the development of the visual servoing procedure at ARL
- Sivan Levi for taking part in the development of the cutting tool at ARL.
- Roee Finkelstein for taking part in the development of the visual servoing procedure at ARL
- Oded Cohen for 3D modeling using range images from multiple viewpoints
- Ofir Karmi for 3D modeling using RGB images from multiple viewpoints
- Omer Nir for developing the close-up modeling procedure at Technion
- Michal Shani for developing the visual servoing procedure at Technion

References

Chaumette, F. (1990). La relation vision-commande: théorie et application a des tâches robotiques. PhD Thesis. Université de Rennes I (France)

Espiau, B. and F. Chaumette (1992). A new approach to visual servoing in robotics. *IEEE Transactions on Robotics and Automation* 8: 313-324.

Lhuillier, M. and L. Quan (2005). Quasi-dense approach to surface reconstruction from uncalibrated images. *IEEE Transactions on Pattern Analysis and Machine Intelligence* 27: 418-433.